Journal of Hazardous Materials 179 (2010) 507–514

Contents lists available at ScienceDirect

Journal of Hazardous Materials

journal homepage: www.elsevier.com/locate/jhazmat

Stabilization and solidification of Pb in cement matrices

Maria A.C. Gollmann[a], Márcia M. da Silva[a], Ângela B. Masuero[b], João Henrique Z. dos Santos[a,*]

[a] Instituto de Química, UFRGS, Av. Bento Gonçalves, 9500 Porto Alegre, 91509-900 RS, Brazil
[b] Escola de Engenharia Civil, UFRGS, Av. Osvaldo Aranha, 99 Porto Alegre, 90035-190 RS, Brazil

ARTICLE INFO

Article history:
Received 24 October 2009
Received in revised form 28 January 2010
Accepted 5 March 2010
Available online 12 March 2010

Keywords:
Cement
Plumb
Stabilization
Solidification
Leaching

ABSTRACT

Pb was incorporated to a series of cement matrices, which were submitted to different testes of solidified/stabilized product. The leaching behaviors of aqueous solution were monitored by graphite furnace atomic absorption spectroscopy (GF-AAS). The mechanical strengths were evaluated by unconfined compressive strength (UCS) at 7 and 28 ages. Data are discussed in terms of metal mobility along the cement block monitored by X-ray fluorescence (XRF) spectrometry. Complementary techniques, namely, diffuse reflectance infrared Fourier transform spectroscopy (DRIFTS), thermal gravimetric analysis (TGA), small angle X-ray scattering (SAXS) and X-ray diffraction spectroscopy (XRD) were employed in the characterization of the modified matrices. The Pb incorporated matrices have shown that a long cure time is more suitable for avoiding metal leaching. At pH 8 lower Pb leaching took place both for both short and long cure time. For a longer cure period there is a decreasing in the compressive strength. TGA and DRIFTS analyses show that the resistance fall observed in the UCS tests in the sample with Pb are not caused by hydration excess. XRF analyses show that there is a lower Ca concentration in the matrix in which Pb was added.

1. Introduction

The growing number of papers and conferences devoted to waste immobilization reflects a genuine need for economic solutions for restoring a safe, clear, green environment. This manner stabilization/solidification (S/S) processes are routinely used for the final treatment of hazardous wastes to reduce contaminant leaching prior to land disposal. Among various types of S/S binders, cement-based systems are the mostly widely used, due to relatively low cost, wide availability and versatility [1–4].

S/S process can be used to convert heavy metals into less mobile form, applicable to several types of wastes which are not suitable to physical, chemical or biological processing [2,5–8]. Industrial activities in the product of materials and chemicals give rise to very large quantities of heavy metal-bearing wastes each year. With the increasing concern regarding environmental pollution and growing interest in sustainable development, the problem of heavy metal immobilization becomes even more significant [9]. Heavy metals are dangerous because they tend to bioaccumulate and can enter into water supply systems by industrial and consumer waste, or even from acidic rain breaking down soils and releasing heavy metals into streams, lakes, rivers, and groundwater. An improper disposal of heavy metals can cause serious environmental and ecological problems. Reduction of impact of those residues is desirable by disposing them into very stable and leaching free conditions. Metals like As, Cr, Pb, Zn, Cu, Hg are issues of a lot of studies and researches [10–15], due to the hazardous effects that can cause to environmental and the human health.

The application of the materials resulting from S/S processes in civil engineering, for instance, depends on the degree of residues leaching, as well as on their structural resistance, minimizing therefore, potential environmental problems. Among metal wastes, those containing Pb represents a serious issue. Pb derivatives are employed in industries for fuel and asphalt. Furthermore, it is also present in mining and metallurgic industries, in processes involving corrosion of metal objects, manufacture of tin pigments, imprint and typographer and plastic incineration (utilized in polymer stabilization) [16]. In humans, Pb exposure can lead to a wide range of biological effects depending on the level and duration of exposure. Various effects occur over a broad range of doses, with the developing fetus and infant being more sensitive than the adult. High levels of exposure may result in toxic biochemical effects in humans which in turn cause problems in the synthesis of haemoglobin, effects on the kidneys, gastrointestinal tract, joints and reproductive system, and acute or chronic damage to the nervous system [17].

A great number of studies have been done about the S/S efficiency in cement matrices. For example, the incorporation of metals (Ni, Pb and Cd) results in a decrease of the $Ca(OH)_2$ content of the cement paste and increases its vulnerability. The leaching rates

* Corresponding author. Tel.: +55 51 3308 7238; fax: +55 51 3308 7304.
E-mail address: jhzds@iq.ufrgs.br (J.H.Z. dos Santos).

0304-3894/$ – see front matter © 2010 Elsevier B.V. All rights reserved.
doi:10.1016/j.jhazmat.2010.03.032

Table 1
Chemical composition and physical properties of the ordinary portland cement.

Composition	Content (%)
SiO_2	26.70
Fe_2O_3	2.27
CaO	52.38
MgO	7.05
Al_2O_3	5.60
SO_3	4.80
Fire lose	2.63
CaO free	0.74
Specific mass (g/cm^3)	3.10

of the metals increased in the following order: Pb ≪ Ni ≪ Cd [18]. Heavy metals (Pb, Cu, Zn, Cd and Mn) added as salts are very effectively immobilized in hydrated matrices (from 99.82 to 99.99%); Cr is an exception immobilized in lower degree (from 85.97 to 93.33%) [10]. The microstructure of cementation wastes containing Pb, Cd, As and Cr was also investigated. The metal leaching in the pH region of 6–8 decreased in the following order: Cr(VI) > Cd(II)Pb(II) > As(V). In another study in which Pb, Zn, Cu, Fe and Mn were immobilized by S/S process, mechanical strength was shown to increase [19].

In a previous study, we evaluated the desorption of lead immobilized into cement and concrete modified matrices. Lead desorbed content was monitored by graphite furnace atomic absorption spectroscopy (GF-AAS) [20], and was shown to be pH dependent. At present we investigated the changes in the cement matrices caused by the incorporation of Pb derivatives. The effect of cement cure time on Pb metal leaching and on the matrix mechanical strengths was evaluated. Data are discussed in terms of metal mobility along the cement block monitored by X-ray fluorescence (XRF) spectrometry. Complementary techniques, namely, diffuse reflectance infrared Fourier transform spectroscopy (DRIFTS), thermal gravimetric analysis (TGA), small angle X-ray scattering (SAXS) and X-ray diffraction spectroscopy (XRD), were employed in the characterization of the modified matrices.

2. Experimental

2.1. Materials and methods

All the tests were carried on using ordinary portland cement (OPC). The chemical composition and physical properties of the employed Portland cement are shown in Table 1. The tests were performed with three different matrices for the control of the effect of the presence of Pb. The first one (reference matrix) consisted solely of cement portland without the metal. In the second one (blank matrix), Pb (10 wt.%) was added. Such matrices were not exposed to pH solutions. Finally, the third one, Pb (10 wt.%) was added and the resulting matrices were submitted to different pH solutions. PbO_2 (Riedel-de Haën) was employed as received. Grain size distribution and physical composition of the sand is included in Table 2. For pH 5, buffer solutions using potassium acid phthalate (Labsynth) 0.1 M and sodium hydroxide (Merck) 0.1 M were employed, while for pH 7 and 8, tris(hydroxymethyl)-amino methane (Merck), 0.05 M and chroridric acid (Labsynth) 0.1 M were used.

Table 2
Grain size distribution and physical composition of the sand.

Aperture (mm)	Retained (%)	Accumulated (%)
4.8 mm	4	4
2.4 mm	9	13
1.2 mm	16	29
600 μm	25	44
300 μm	35	89
150 μm	11	100
<150 μm	0	100
Specific mass = 2.65 g/cm^3		

2.2. Solidification and cure procedure

PbO_2 and cement (90% OPC + 10% Pb wastes) were mixed with water at a water/solid (cement and Pb wastes) ratio (W/S) of 0.6, which was established based on tests carried out according to the Brazilian Standards NBR-5738 [21]. Before the rupture tests the relationship water–cement was evaluated. It is worth noting that the water–cement ratios as well as the curing conditions, type of binder, and use of mineral and chemical admixtures have significant effects on the value of the total porosity and the pore size distribution [22].

Samples were introduced into metal cylindrical mounds measuring 50 mm diameter × 100 mm height. Air bubbles in the paste were removed by tapping the mold with approximately 40 hits (for about 1 min). The molds were exposed to humid air (90 ± 2% relative humidity). The samples were cured at approximately 23 ± 2 °C for 7 and 28 days, in agreement with the NBR-5738. After the period of curing the samples were unmolded.

2.3. Leaching test

The leaching test consisted of putting blocks into a PVC pot, immersed in water solution with different pH (pH 5, 7 and 8). The blocks continued being cured in these solutions for periods of 7, 14, 21 and 28 days, after staying in humid ambient. The liquid/solid (L/S) ratio was 4, and the static leaching condition was employed. A set of five blocks were used for compression strength tests, established by the Brazilian Standards NBR-5739 [23]. For each curing duration, one block of each pH solution, one reference block and one blank block were submitted to the compression strength test which were carried in triplicate. Therefore, 15 blocks were broken for each cure period. During all tests, the pH of the solution was weekly monitored.

2.4. Unconfined compressive strength (UCS) tests

UCS tests were undertaken with the samples using a SHIMADZU machine, model Autograph UH2000 KNG, capacity 40–2000 kN, velocity 30 kN/min (0.254 MPa/s). The top of the samples was capped with Masonite® to limit the effect of cracking. Loading was increased up to reaching the maximum amount and visible cracks appearance. The compressive strength was calculated as the maximum applied force loading divided by the cross-sectional area. All tests were established by the Brazilian Standards NBR-5739.

2.5. Graphite furnace atomic absorption spectroscopy (GF-AAS)

The concentration of Pb ions in the solutions was measured by GF-AAS at 217.0 nm. The metal content was determined in triplicate. For each sample, the mean of three AAS measurements was recorded. The furnace program used in the analysis is showed in Table 3.

2.6. Thermogravimetry (TGA)

The thermogravimetric curves were recorded with a TGA Q5000 V3.5 Build 252 apparatus. The samples were heated from room temperature to 400 °C at a heating rate of 0.33 °C s^{-1} under nitrogen flow (1 cm^3 s^{-1}).

Table 3
Graphite furnace heating program employed for analysis.

Steps	T (°C)	Time (s)		Argon flow rate (mL min^{-1})
		Ramp	Hold time	
Drying	140	5	45	300
Pyrolysis	900	100	30	300
Atomization	1900	FP	6	0
Cleaning	2100	1000	5	300

FP = full power.

2.7. Diffuse reflectance infrared Fourier transform spectroscopy (DRIFTS)

DRIFTS measurements were performed on a Bomem Instrument, in reflectance mode. The spectra were by coadding 32 scans at a spectral resolution of 4 cm^{-1}. Samples were analyzed as powders.

2.8. X-ray diffraction (XRD) spectroscopy

The crystal structure and phase composition of the solids were analyzed by powder X-ray diffraction, using a Rigaku X-ray diffractometer, model DMAX, with Cu Kα radiation (λ = 0.154178 nm), using an accelerating voltage of 40 kV. Samples were analyzed as powders.

2.9. X-ray fluorescence (XRF) spectrometry

The XRF analyses were carried out in a Rigaku (RIX 3100) wavelength dispersive X-ray fluorescence spectrometer equipped with a Rh X-ray tube, 4 kW generator and 8 position crystal changer. The spectrometer was interfaced to a PC with a RIX for Windows software. Operating conditions and spectrometer parameters are described in Table 4. For the analyses, samples were collected from the external part and bulk (ca. 25 mm) of the blocks.

2.10. Small angle X-ray scattering (SAXS)

The SAXS experiments were carried out using synchrotron radiation at LNLS (Campinas, Brazil) with a wavelength k = 1.488 nm. The beam was monochromatized by a silicon monochromator and collimated by a set of slits defining a pin-hole geometry. A solid-stated CCD detector (MAR 160) was used to collect two-dimensional (2D) images with 2048 × 2048 pixels located at 6752.5 mm of the sample. The q-range of the scattering curves was 0.02 nm^{-1} ≤ q ≤ 60.49 nm^{-1}, where q is the scattering vector ($q = 4\pi/\lambda \sin(\theta/2)$). The data were corrected for sample transmission and background scattering using an empty cell as reference. Samples were placed in stainless steel sample holders closed by two mica windows.

3. Results and discussion

In the following discussion, the label S states for sample, SB for blank (with Pb), SR for reference (without Pb) and the numbers 5, 7 and 8 are used to describe the pH of the solutions. Thereafter, the letter S is used for short (7 days) and L for long (28 days) cure time. Then, for instance, S5-L means a sample with Pb that was cured in humid air for 28 days and then was exposed to a pH 5 solution. The samples SB and SR were not exposed to pH solutions, and they served to evaluate the effect that the Pb addition caused in the cement matrices resistance.

Table 4
X-ray fluorescence operating conditions and spectrometer parameters.

Element	Crystal	Spectral line	2θ (°)	Time (s)	Detector
Ca	LiF 200	Kα	113.5	40	F-PC
Al	PET (pentaerytritol)	Kα	145.2	40	F-PC
[a]Fe	LiF 200	Kα	57.5	40	SC NaI (Tl)
[a]Pb	LiF 200	Lβ	28.2	40	SC NaI (Tl)

bg = background; F-PC = flow proportional counter; SC = scintillation detector.
[a] Compton scattering matrix correction.

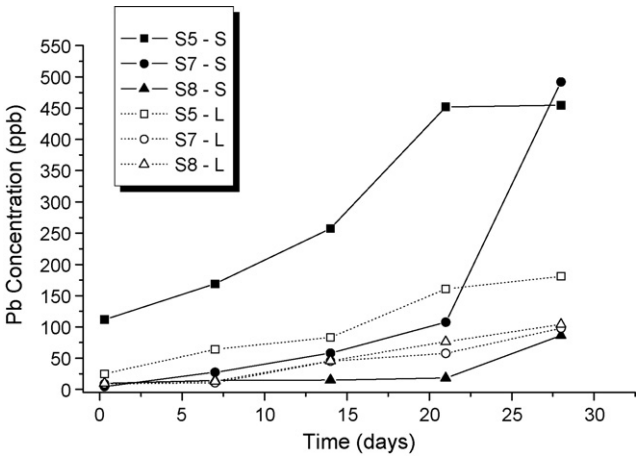

Fig. 1. Metal leaching at different pH solutions, for blocks submitted to 7 (S) and 28 (L) days of cure.

In this study, the effect of the cure time on metal leaching and block mechanical strength was evaluated. For each rupture, samples were collected at different pH solutions. Then, the blocks were draw back from the solutions and submitted to the evaluation of strength.

Fig. 1 shows the amount of leached Pb from the cement blocks submitted to 7 and 28 days of cure in humid air.

The results of the leaching test demonstrated that in blocks with long cure, the amount of leached Pb was lower than that observed in the case of short one. The exception was S8-S, which was shown to be as efficient as the blocks with long cure time. For the other solutions containing blocks with short cure time, the Pb leached amount lain around 75–80% higher than those bearing blocks submitted to longer cure time (see S5 and S7, respectively). For longer periods of cure, all blocks were shown to be efficient for the metal retention, because the leached metal amount remained in levels which were acceptable in agreement with the Brazilian Standards NBR 10004/1987 [24]. It is worth noting that S5 presented the worst results, independent of the cure time, suggesting that acid pH can cause damage for these blocks in terms of Pb leaching.

Concerning the pH of such systems, it is observed that basic pH affords lower leaching content in relationship to the acid pH. For matrices submitted to pH 7, a distinct behavior was observed that depends on the cure time. Short cure time engenders a higher Pb leaching for this pH, while long cure time affords a smaller Pb content in solution.

These results reveal the potentiality of using theses blocks in terms of environmental safety. Nevertheless, from the point of view of technological application, it is necessary to evaluate their resistance by means of unconfined compressive strength (UCS) tests. Therefore, after collecting the samples for FG-AAS analyses, each block was submitted to the UCS test. This test permits an evaluation about the potential efficiency of the blocks for retention of the metal and its influence on the resistance of these blocks. The results of the compressive strength for blocks with short and long cure are showed in Tables 5 and 6, respectively.

Two factors are observed in the results of compressive strength tests. In general, blocks with a longer cure period showed higher

Table 5
Mechanical compressive strengths (kgf/cm^2) for the blocks: SB, SR, S5, S7 and S8; with 7 days of setting times.

Time (days)	Mechanical compressive strength (kgf/cm^2)				
Cure period	SB-S	SR-S	S5-S	S7-S	S8-S
7	32.07	31.67	29.75	38.10	36.62
14	29.30	32.00	29.82	28.14	37.13
21	39.73	32.00	37.69	32.67	29.63
28	45.27	42.26	33.34	26.49	26.33

Table 6
Mechanical compressive strengths (kgf/cm^2) for the matrix: SB, SR, S5, S7 and S8; with 28 days of setting times.

Time (days)	Mechanical compressive strength (kgf/cm^2)				
Cure period	SB-L	SR-L	S5-L	S7-L	S8-L
7	29.62	37.20	33.69	27.70	26.60
14	35.48	37.75	27.59	28.10	29.45
21	32.87	43.15	29.98	36.40	27.50
28	30.00	45.75	21.73	35.56	29.17

resistance. This observation is common in studies and experiments dealing with concrete or cement strength reported in literature [22,25–27]. In our study the results obtained for SR confirm this behavior.

On the other hand, the obtained data showed that in blocks SB-S the strength is comparable or, in almost all the setting data, is higher than that observed for blocks SR-S. This suggests that the Pb addition is favorable, because it gives an additional strength for the blocks in short cure period (Table 5). For the same period of cure time the blocks which suffer the action of the pH, exhibit, independently of the pH, a smaller strength, which suggests that the external environment reduces the block strength. For the first ages, 7 and 14 days, the pH effect is smaller, but for longer periods the pH effect is observed and causes a significant decrease in the strength.

For longer cure period (Table 6), the negative metal effect is clear. It is observed that the strength of the SB-L blocks decreased in relationship to the SR-L ones. In this case, it is observed a trend in which there is an increasing in the strength in the first ages (7 and 14 days), followed by a decreasing after 21 and 28 days of the curing. Similar results have been reported in the literature in the case of hydration kinetics studies [28]. Furthermore, the authors observed that after cure time, heavy metals within cement matrices can influence on the mechanical strength and permeability of the matrices.

In the present study, these results demanded a deeper analysis of the block microstructure aiming at investigating the role of Pb within these systems. A possibility is that the metal is acting in the block structure under two forms: by engendering higher water

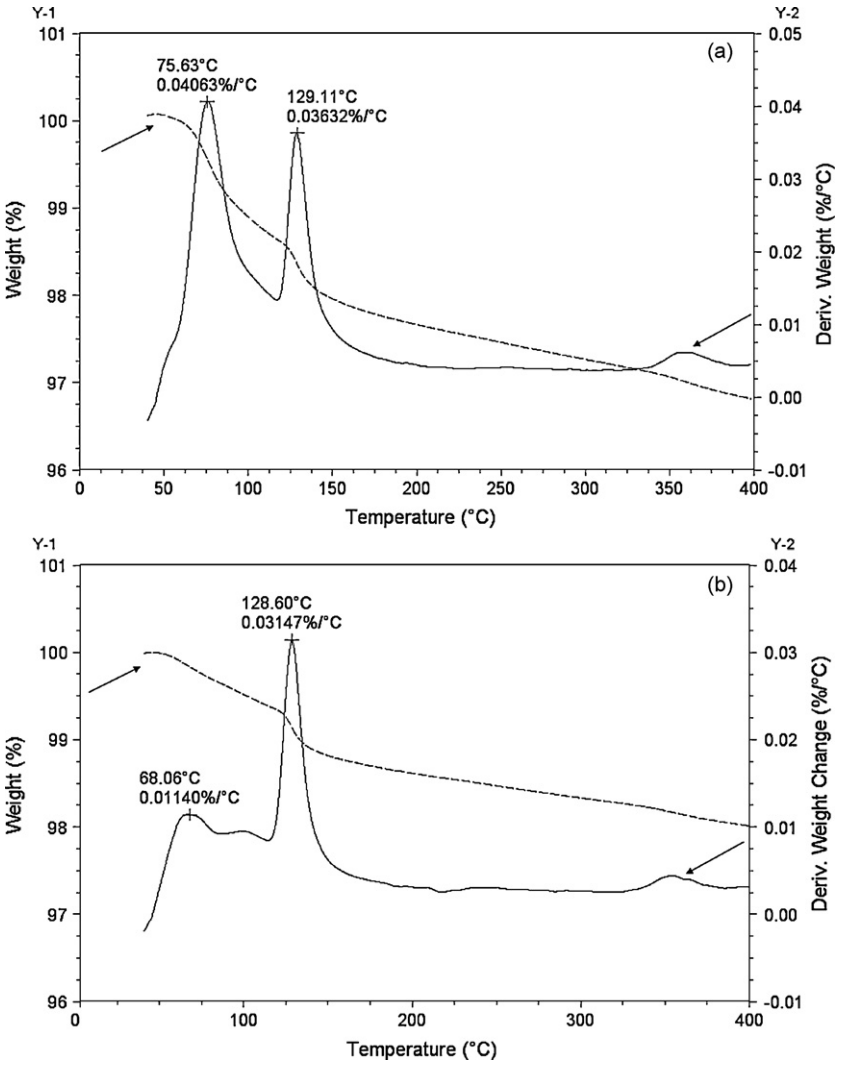

Fig. 2. TGA thermograms of cement-water systems: (a) in the presence and (b) in the absence of Pb.

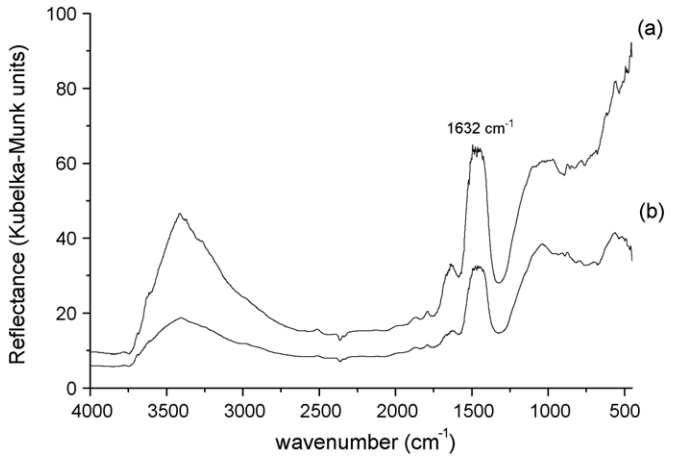

Fig. 3. DRIFTS of cement-water system: (a) in the absence and (b) in the presence of Pb.

incorporation or by causing an isomorphic substitution between the heavy metal and some elements constituents of the cement matrix.

In the first case metal addition could generate higher water incorporation in the mixing. This fact would also cause the resistance fall to longer curing periods. The hydration excess has a negative influence in the cement and mortar mixing [29–31]. Hydrolysis yields an important increase in cement paste porosity, owing to (i) the leaching of hydrate such as calcium hydroxide (i.e. portlandite, $Ca(OH)_2$) and (ii) the decalcification of the calcium silicate hydrates ($3CaO{\cdot}2SiO_2{\cdot}xH_2O$, $x \cong 3$). Note that the porosity can favor the mobility of the components towards to the external solution, thus favoring cement degradation reactions [32]. In order to understanding the behavior and its influence of Pb in the paste hydration, analyses of the blocks by TGA were performed. The samples were heated up to 400 °C in order to quantify the percentage of incorporated water in systems containing or not Pb (Fig. 2).

Fig. 2 shows that the loss of water in the sample water–cement–Pb is practically the same when compared to sample constituted of water–cement (0.08 *versus* 0.04%), being agreement with data reported in the literature [33–35]. Such results suggest that the presence of Pb did not afford retention of water within the matrix. The water interaction with these blocks was further investigated by DRIFTS, which provided information about the uppermost surface (see Fig. 3).

Fig. 3 shows the deformation $\delta_{(OH)}$ band intensity centered at 1632 cm^{-1}, associated to the presence of water molecules detected in the sample containing Pb. These results confirm the behavior depicted in TGA thermogram. The presence of Pb in cement matrices seems not to afford an increasing in water content, which could be responsible for block cracking.

Another possibility of the effect on the matrix resistance resides in the isomorphic substitution between Pb and some element constituents of the matrix, such as Ca.

Various studies have evaluated the interactions of Pb and Ca with the cement matrix. For example, studies have postulated Pb to be either adsorbed onto the calcium silicate hydrated matrix of cement [36,37] or precipitated as Pb silicate [38,39]. The formation of leadhilite (lead carbonate sulfate hydroxide, $Pb_4SO_4(CO_3)_2(OH)_2$), lead carbonate hydroxide hydrate ($3PbCO_3{\cdot}2Pb(OH)_2{\cdot}H_2O$) and two others unidentified lead salts was appointed by another research [40]. These products were formed by chemical incorporation/adsorption of re-dissolved Pb species. The structure of cementation wastes containing Pb(II) and others metals was evaluated. Pb ions were homogeneously dispersed in the calcium silicate hydrated matrix by adsorption or precipitation with calcium or silicate compounds present in the cement [8]. Other study suggests that Pb generally replace calcium in the cement hydrates phases [41].

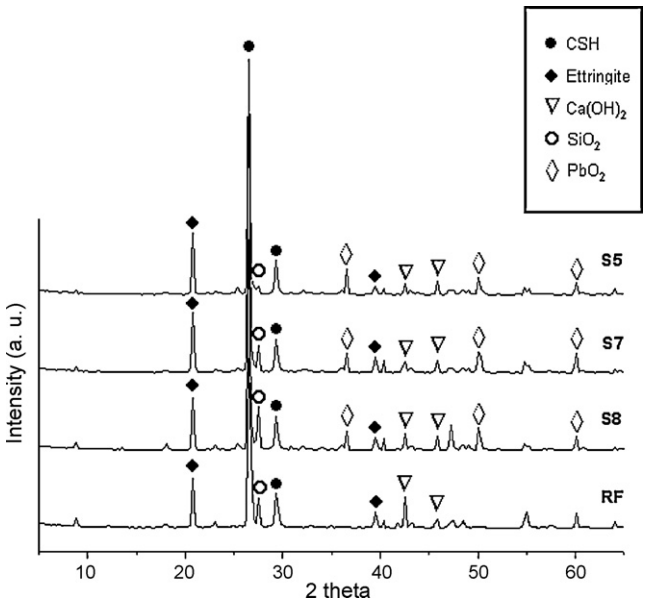

Fig. 4. XRD patterns of SR, S8, S7 and S5 samples.

In order to understand the mortar structure and the differences that Pb addition and the external medium may cause to the matrices, XRD analyses were performed in the blocks after pH submission (Fig. 4).

According to the diffractograms, the detected signals can be assigned to calcite ($CaCO_3$), calcium silicates hydrates ($3CaO{\cdot}2SiO_2{\cdot}xH_2O$, $x \cong 3$), ettringite ($6CaO{\cdot}Al_2O_3{\cdot}3SO_3{\cdot}32H_2O$), portlandite ($Ca(OH_2)$) and SiO_2, those result is according with the literature [30–33]. In samples S8, S7 and S5, it is possible to observe the presence of plattnerite (PbO_2). Datas obtained from XRD techniques show that leaching does not measurably affect the crystalline structure of the solidified waste sample, as reported in some studies [33–35,42]. However, changes in the morphology and cement composition can be analyzed. In order to understand the blocks microstructure and the possible composition changes that Pb addition causes in these systems, XRF analyses were performed. After the mechanical strength tests of those matrices, samples were collected from the external and bulk parts of the blocks. Ca, Al and Fe contents were monitored due to their importance in the cement and mortar. Element content was expressed in terms of metal/Si ratio (M/Si), since Si (as SiO_2) is stable under such pH conditions. The results were expressed in term of rate intensity and are showed in Table 7.

The XRF analyses show that the cement matrices are homogeneous (see Table 7 SR matrix) and that there is a higher Ca concentration in the matrix in which Pb was not added and that are not exposed to aggressive medium. Cement has a very complex structure, but it is known that Ca is one of the main

Table 7
Metal/Si ratio in concrete matrix measured by XRF.

Sample	Ca/Si	Al/Si	Fe/Si	Pb/Si
S5-L external	1.34	0.04	0.17	0.37
S5-L bulk	1.75	0.05	0.16	0.39
S8-L external	1.58	0.05	0.14	0.40
S8-L bulk	1.75	0.05	0.16	0.40
SR external	6.37	0.01	0.46	–
SR bulk	6.02	0.06	0.44	–

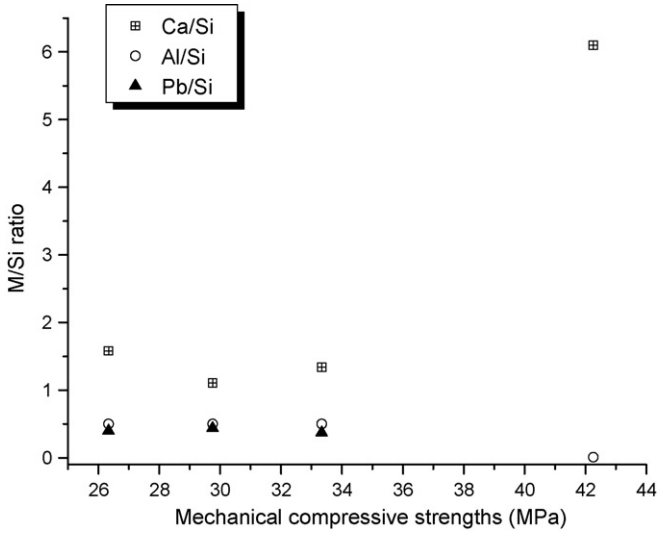

Fig. 5. Relationship between compressive strengths and matrix metal content M/Si, M = Ca, Al, Pb (bulk and external surface) in mortar matrices.

constituents of the cement matrices. The mineral composition is basically constituted of alite or tricalcium silicate $(CaO)_3SiO_5$ belite or dicalcium silicate $CaO)_2SiO_2$, tricalcium aluminate $(CaO)_3Al_2O_6$ and ferrite phase or tetracalcium aluminoferrite $(CaO)_4Al_2O_3Fe_2O_3$. The respective percentage is roughly 45 and 60%, 15 and 30%, 6 and 12%, and 6 and 8% [29,43,44]. The major product of silicate phase, hydrated calcium silicate ($CaOSiO_2{\cdot}H_2O$) is one of the main constituents of the cement matrices, and it is the main responsible for its resistance [29,43]. Therefore, a relationship between the compressive strength and the matrices metal content was carried on. The results are shown in Fig. 5.

The results suggest that the Ca/Si ratio reduction can contributes to resistance decrease. Calcium leaching is a degradation process that consists in the progressive dissolution of the cement paste as a consequence of the migration of the calcium ions to the aggressive solution. This phenomenon is normally observed in aggressive solutions [5,8,14,15], as in the present case. In several studies it was observed that the pH increasing causes a solubility of Ca^{2+} in

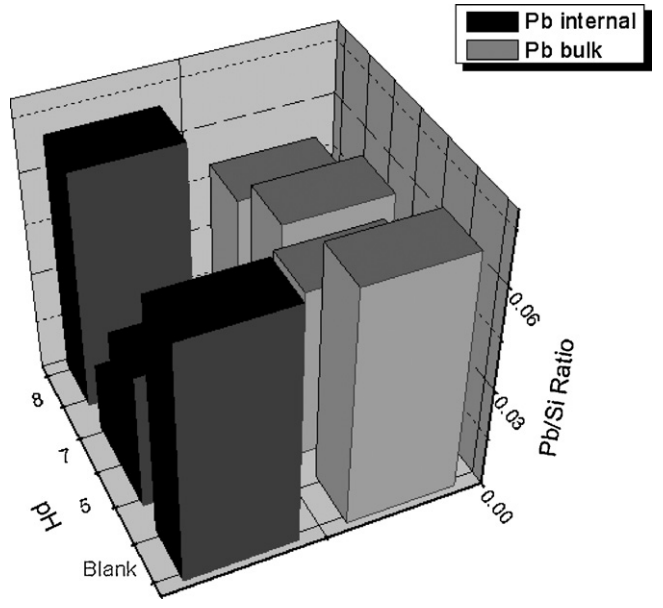

Fig. 6. Pb/Si ratio in the bulk and external surface of the matrices submitted to different pH.

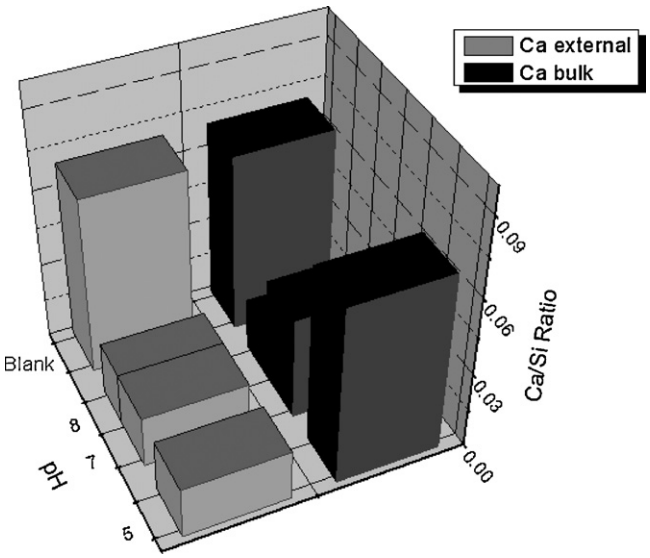

Fig. 7. Ca/Si ratio in the bulk and external surface of the matrices submitted to different pH.

the calcite/portlandite phase [45,46]. The lead behavior is different: when the pH increases there is a trend to form oxides (such as PbO_2, for example), while for pH decreasing, the generation of Pb^{2+} is favored [47]. Thus, the leaching effect played by the solutions was then monitored by expressing the Pb/Si and Ca/Si ratio, detected in the bulk and external surface of the matrices, after submission of the matrices to different pH solutions, as illustrated in Figs. 6 and 7, respectively.

According to Fig. 6, the Pb content in the bulk and external surfaces is roughly the same for the matrices which were not exposed to pH solutions (blank). This result suggests that Pb was initially homogeneously distributed along the matrices, and different distribution was achieved after the contact with the pH solutions. For the bulk surface, Pb content seems to be much reduced in acid pH, probably due to migration towards the external medium. Nevertheless, alkaline medium (pH 8) seems not to affect the Pb/Si ratio, if compared to the blank. Concerning the external surface, the variation along the tested pH seems to be less significant, probably due to compensation of Pb migrated from the bulk to the external matrices surface. Fig. 7 shows the results expressed for Ca/Si ratio.

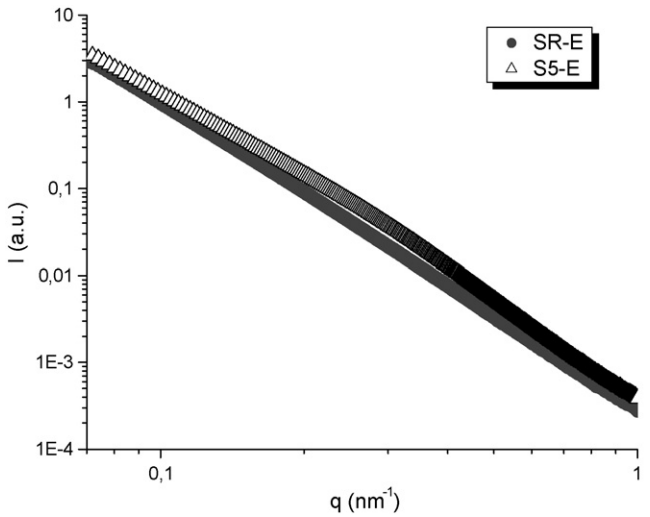

Fig. 8. SAXS profiles plotted as $I(q) \times q$ to cement matrices RF and S8, external surface.

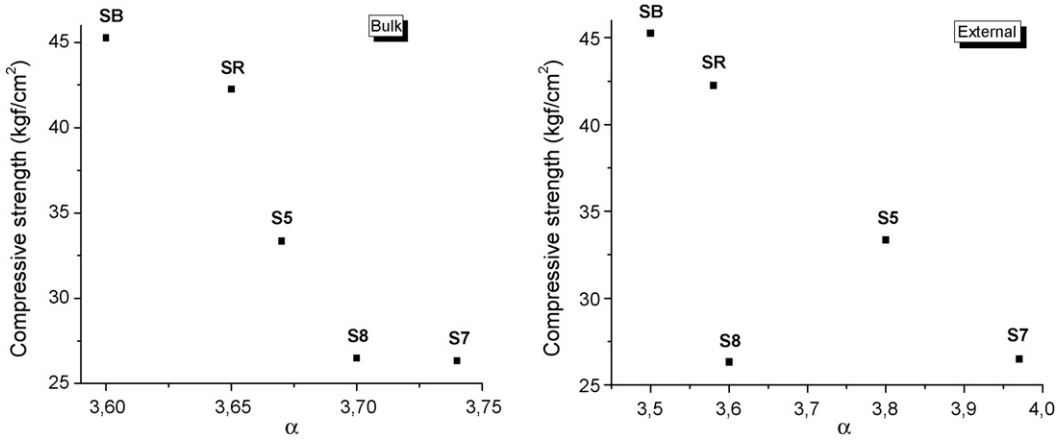

Fig. 9. Correlation between fractal coefficient (α) and of the resistance.

Similarly to the Pb leaching behavior, the blank samples suggest a uniform distribution of Ca both along the bulk and external surfaces. Nevertheless, Ca seems to be more prone to leaching under these investigated conditions, considering that a reduction in Ca is observed both in the external surface, as in the bulk one. Conversely to Pb, in the bulk surface, Ca content is lower in pH 7 and 8 than in pH 5. It can be explained because the pH of the solution increases very quickly, although the pH have been monitored weekly.

It is important to point out that the Pb content in the external surface of cement matrices exposed to pH solutions are higher than Ca one under the same conditions. In the bulk surface, the content is comparable for all investigated pH values, excepting for pH 5, in which Ca content is superior. The results of XRF indicate Pb migration to the external surfaces in matrices of pH 5, 7 and 8, and its migration rate increases as pH decreases. In the case of Ca, lower content was observed in the external surface for all the systems. Nevertheless, its migration from the bulk surface seems to be more affected as the pH increases, probably due to the enhancement of Ca^{2+} solubility in the calcite/portlandite phase, as previously commented.

In the present study, fractal geometry of the cement matrix was determined by small angle X-ray scattering (SAXS). Fig. 8 shows the SAXS curves, plotted as $I(q) \times q$, for the cement matrices SR and S5 (E – external surface).

Taking into account the q intermediate region in the SAXS curve, α coefficient values (slope) were calculated for the different systems: SR, SB, S8, S7 and S5, bulk and external surfaces. This coefficient is related to the fractal geometry of the matrices, as shown in Table 8.

According to Table 8, SAXS results show that there are two regions in the matrix: a denser one (3.6) and another one less dense (3.03). In the matrix SR (without Pb), only one region is depicted indicating that the two observed regions might be resulting from Pb addition. It is worth noting that in the case of the bulk surface, submitted to pH 8 (S8), only one region is detected, being in the agreement with XRF results (Fig. 8), which content was much similar to that measured in the Blank.

Table 8
Alpha values of the bulk and external part of the matrixes.

Sample	Bulk		External surface	
SR	3.60		3.58	
SB	3.65	3.03	3.5	3.15
S5	3.67	3.31	3.8	3.35
S7	3.70	3.20	3.97	3.31
S8	3.74		3.6	3.13

In general, the increasing in pH engenders enhancement in the mortar density. The pH influences in the density of the matrix, probably because the continuous contact with the aggressive external ambient.

Fig. 9 presents the correlations between the compressive strength and fractal geometry (α) values determined by SAXS data for internal and external part are analyzed.

According Fig. 9, the behavior in both bulk and external surface is similar. The presence of Pb affects both the strength and α values. The reduction is sharper in the case of the external surface, which is most exposed to the pH solution.

4. Conclusion

In the present study, it was observed that Pb stabilization and solidification in mortar is possible. The introduction of Pb into the matrices engenders a reduction in the resistance, not by hydration excess, but rather by an exchange reaction between Pb and the phases of the cement. Furthermore, the stability of the resulting mortars is sensitive to the external environment. Ca leaching, in basic medium, seems to be the main cause which contributes to resistance decreasing in the matrices. Therefore, solutions with pH closer to neutral are the most suitable for the matrices application when Pb is present in their manufacture. Then, Pb stabilization and solidification in mortars can be a suitable procedure to immobilize Pb residues, if such matrices are used or kept in environments which are not exposed to very aggressive media in terms of pH values.

Acknowledgments

This project was partially financed by CNPq. M.A. Gollmann thanks CNPq for the grant. The authors are thankful to LNLS (Project D11A SAXS1 #5296) for measurements in the SAXS beamline.

References

[1] P. Gong, P.L. Bishop, Evaluation of organics leaching from solidification/stabilization hazardous wastes using a powder reactivated carbon additive, Environ. Technol. 24 (2003) 445–455.
[2] J.R. Conner, Chemical Fixation and Solidification of Hazardous Wastes, Van Nostrand, Reihold, New York, 1990.
[3] P. Ubbrìaco, D. Calabrase, Solidification and stabilization of cement paste containing fly ash from municipal solid waste, Thermochim. Acta 321 (1998) 143–150.
[4] M.L. Murat, Y. Yüksel, Potential use of fly ash bentonite mixture as liner or cover as waste disposal areas, Environ. Geol. 40 (2001) 1316–1324.
[5] Y.C. Yang, M.G. Shaaban, H.B. Mahmud, Chemical stabilization of scrap metal yard contaminated soil using ordinary Portland cement: strength and leachability aspects, Build. Environ. 42 (2007) 794–802.

[6] G. Qian, Y. Cao, P. Chui, J. Tay, Utilization of MSWI fly ash stabilization/solidification of industrial waste sludge, J. Hazard. Mater. 129 (2006) 274–281.
[7] M.C. Ruiz, A. Irabien, Environmental behavior of stabilization foundry sludge, J. Hazard. Mater. 109 (2004) 45–52.
[8] C.E. Halim, R. Amal, D. Beydoun, J.A. Scott, G. Low, Implications of the structure of cementation wastes containing Pb(II), Cd(II), As(V) and Cr(VI) in the leaching of metals, Cement Concr. Res. 34 (2004) 1093–1102.
[9] J. Zhang, J.L. Provis, D. Fenga, J.S.J. van, Deventera, Geopolymers for immobilization of Cr^{6+}, Cd^{2+}, and Pb^{2+}, J. Hazard. Mater. 157 (2008) 587–598.
[10] Z. Giergiczny, A. Król, Immobilization of heavy metals (Pb, Cu, Cr, Zn, Cd, Mn) in the mineral additions containing concrete composites, J. Hazard. Mater. 160 (2008) 247–255.
[11] S. Peysson, J. Péra, M. Chabannet, Immobilization of heavy metals by calcium sulfoaluminate cement, Cement Concr. Res. 35 (2005) 2261–2270.
[12] A. Reyad, Shawabkeh, Solidification and stabilization of cadmium ions in sand–cement–clay mixture, J. Hazard. Mater. B 125 (2005) 237–243.
[13] A. Marion, M. De Lanéve, A. De Grauw, Study of the leaching behaviour of paving concrete quantification of heavy metal content in leachates issued from tank test using demineralized water, Cement Concr. Res. 35 (2005) 951–957.
[14] R. Dewil, J. Baeyens, L. Appels, Enhancing the use of waste activated sludge as bio-fuel through selectively reducing its heavy metal content, J. Hazard. Mater. 144 (2007) 703–707.
[15] C.E. Halima, S.A. Short, J.A. Scott, R. Amal, G. Low, Modelling the leaching of Pb, Cd, As, and Cr from cementations waste using PHREEQC, J. Hazard. Mater. A 125 (2005) 45–61.
[16] N.N. Greenwood, A. Earnshaw, Chemistry of the Elements, Butterworth Heinemann, Oxford, 1997.
[17] Available: http://www.lenntech.com/heavy-metals.htm.
[18] D. Bonen, L.S. Shondeep, The effects of simulated environmental attack on immobilization of heavy metals doped in cement-based materials, J. Hazard. Mater. 40 (1995) 321–335.
[19] R. Malviya, R. Chaudhary, Leaching behaviour and immobilization of heavy metals in solidified/stabilized products, J. Hazard. Mater. B 137 (2006) 207–217.
[20] M.A.C. Gollmann, A. Walesko, A. Fisch, F.C. Stedile, M.M. da Silva, J.H.Z. dos Santos, R.M. Lattuada, Evaluation of lead desorption form cement matrices, J. Environ. Sci. Health A 42 (2007) 1183–1189.
[21] Brazilian Standards NBR-5738.
[22] H.N. Atahan, O.N. Oktar, M.A. Tasdemir, Effects of water–cement ratio and curing time on the critical pore width of hardened cement paste, Construct. Build. Mater. 23 (2009) 1196–1200.
[23] Brazilian Standards NBR-5739.
[24] Brazilian Standards NBR 10004/1987.
[25] J. Yang, B. Xiao, Development of unsintered construction materials from red mud wastes produced in the sintering alumina process, Construct. Build. Mater. 22 (2008) 2299–2307.
[26] T. Lee, W. Wang, P. Shih, Slag-cement mortar made with cements and slag vitrified from MSWI fly-ash/scrubber-ash and glass frit, Construct. Build. Mater. 22 (2008) 1914–1921.
[27] J.J. Gaitero, I. Campillo, A. Guerrero, Reduction of the calcium leaching rate of cement paste by addition of silica nanoparticles, Cement Concr. Res. 38 (2008) 1112–1118.
[28] I. Elkhadiri, F. Puertas, The effect of curing temperature on sulphate-resistant cement hydration and strength, Construct. Build. Mater. 22 (2008) 1331–1341.
[29] Q.Y. Chen, M. Tyrer, C.D. Hills, X.M. Yang, P. Carey, Immobilization of heavy metal in cement-based solidification/stabilisation: a review, Waste Manage. 29 (2009) 390–403.
[30] M. Pei, Z. Wang, W. Li, J. Zhang, Q. Pan, X. Qin, The properties of cementitious materials superplasticized with two superplasticizers based on aminosulfonate–phenol–formaldehyde, Construct. Build. Mater. 22 (2008) 2382–2385.
[31] M. Cyr, P. Lawrence, E. Ringot, Mineral admixtures in mortars quantification of the physical effects of inert materials on short-term hydration, Cement Concr. Res. 35 (2005) 719–730.
[32] C. Lampris, J.A. Stegemann, C.R. Cheeseman, Solidification/stabilisation of air pollution control residues using Portland cement: physical properties and chloride leaching, Waste Manage. 29 (2009) 1067–1075.
[33] M. Katsioti, N. Katsiotis, G. Rouni, D. Bakirtzis, M. Loizidou, The effect of bentonite/cement mortar for the stabilization/solidification of sewage sludge containing heavy metals, Cement Concr. Compos. 30 (2008) 1013–1019.
[34] N. Marinoni, A. Pavese, M. Voltolini, M. Merlini, Long-term leaching test in concretes: an X-ray powder diffraction study, Cem. Concr. Compos. 30 (2008) 700–705.
[35] M. Katsioti, D. Gkanis, P. Pipilikaki, A. Sakellariou, A. Papathanasiou, C. Teas, E. Chaniotakis, P. Moundoulas, A. Moropoulou, Study of the substitution of limestone filler with pozzolanic additives in mortars, Construct. Build. Mater. 23 (2009) 1960–1965.
[36] K.Y. Cheng, Controlling mechanism of metals release from cement-based waste form in acid acetic solution, PhD Thesis, University of Cincinnati, Cincinnati, OH, 1991.
[37] D.L. Cocke, The binding chemistry and leaching mechanisms of hazardous substances in cementitions solidification/stabilization system, J. Hazard. Mater. 24 (1990) 231–253.
[38] M.S.Y. Bhatty, Fixation of metallic ions in portland cement, in: Proceeding 4th National Conferences on Hazardous Materials, Portland Cement Association, Skokie, IL, 1987, pp. 140–145.
[39] P.L. Bishop, Leaching of inorganic hazardous constituents from stabilization/solidification hazardous wastes, Waste Hazard. Mater. 5 (2) (1988) 129–143.
[40] D. Lee, Formation of leadhillite and calcium lead silicate hydrated (C–Pb–S–H) in the solidification/stabilization of lead contaminants, Chemistry 66 (2007) 1727–1733.
[41] M.L.D. Gougar, B.E. Scheetz, D.M. Roy, Ettringite and C–S–H portland cement phases for waste ion immobilization: a review, Waste Manage. 16 (4) (1996) 295–303.
[42] G.N. Salaita, P.H. Tate, Spectroscopic and microscopic characterization of portland cement based unleached and leached solidification waste, Appl. Surf. Sci. 133 (1998) 33–46.
[43] Y. Tezuka, Guia de utilização de cimentos hidráulicos, Brazilian Society of Portland Cement, publication São Paulo, 1988.
[44] A. Leemann, B. Lothenbach, The influence of potassium–sodium ratio in cement on concrete expansion due to alkali-aggregate reaction, Cement Concr. Res. 38 (2008) 1162–1168.
[45] E.J. Reardon, R. Fagan, The calcite/portlandite phase boundary: enhanced calcite solubility at high pH, Appl. Geochem. 15 (2000) 327–335.
[46] J. Duchesne, E.J. Reardon, Measurement and prediction of portlandite solubility in alkali solutions, Cement Concr. Res. 25 (1995) 1043–1053.
[47] W. Stumm, J.J. Morgan, Aquatic Chemistry Equilibria and Rates in Natural Waters, Wiley, 1996.